In-medium full-folding optical model for nucleon-nucleus elastic scattering

H. F. Arellano,[1,2] F. A. Brieva,[1] and W. G. Love[2]
[1]*Departamento de Física, Facultad de Ciencias Físicas y Matemáticas, Universidad de Chile, Casilla 487-3, Santiago, Chile*
[2]*Department of Physics and Astronomy, University of Georgia, Athens, Georgia 30602*
(Received 21 February 1995)

We develop an approach for incorporating both medium and off-shell effects in the calculation of full-folding nucleon-nucleus optical potentials for elastic scattering. The approach is based on a flexible scheme for calculating the nucleon-nucleon effective interaction in the nuclear medium. Using this scheme, we calculate a fully off-shell, energy-dependent effective force which includes effects arising from Pauli blocking and the nuclear mean field via an interacting nuclear matter model. Calculations of the elastic scattering observables for p+^{40}Ca and for p+^{208}Pb at energies between 30 and 400 MeV are presented and discussed. We also study total cross sections for neutron scattering off ^{40}Ca, ^{90}Zr, and ^{208}Pb in the 5 – 400 MeV energy range. The theory gives a reasonable overall description of the data in the energy range under study.

PACS number(s): 24.10.Ht, 13.75.Cs, 21.30.+y, 25.40.Cm

I. INTRODUCTION

Elastic nucleon scattering from nuclei continues to challenge and advance our understanding of the basic microscopic mechanisms which determine the nonrelativistic nuclear dynamics [1]. The ability to include explicitly on- and off-shell effects [2–4] and the presence of a bound-state singularity [5] in the underlying internucleon force when calculating the scattering observables, mainly in the 200–400 MeV energy range, has provided a new way to better understand the scattering data, particularly spin observables. The simple phenomenological picture of the interaction of nucleons with nuclei has, to a large extent, given way to microscopic theories characterized by the calculation of the elastic channel average nucleon-nucleus (NA) interaction, the optical potential model.

To first order, a common assumption underlying the most recent intermediate energy nonrelativistic optical potential models is that the effective nucleon-nucleon (NN) force can be approximated by the free NN t matrix [1–4]. The expectation is that, at sufficiently high incident energies, medium effects such as Pauli blocking and the nuclear mean field are of secondary importance in determining the scattering observables. Based on this assumption, two main lines of research have been developed to evaluate the leading term of the nucleon-nucleus optical potential corresponding to the single scattering approximation in a multiple scattering series expansion. One of them is the full-folding model [4] which treats explicitly the off-shell behavior *and* energy dependence of the NN t matrix when convoluting the effective internucleon force with the target ground state mixed density. The other approach is based on an expansion about the so called "$t\rho$" approximation [1–3,6]. In these $t\rho$ models the assumption made is that the off-shell and energy dependence of the NN t matrix is weak enough to allow, in momentum space, a factorized expression for the optical potential as the product of the target density with an on-shell or off-shell NN effective force. Comparisons of the two approaches show some interesting differences, with the full-folding model calculations giving a better description of the data for energies between 200 and 400 MeV. Recent full-folding results show, however, that the NN free t matrix approximation for the effective NN force is rather poor at 200 MeV and below [5]. Indeed, a careful treatment of the pole singularity in the deuteron channel of the t matrix leads to results that make the validity of the $t\rho$ approach questionable as a reasonable starting point to which medium and higher order contributions should be added.

In order to improve our current description of NA scattering beyond the free t-matrix approach and extend the range of energies where the microscopic optical potential is accurate for describing data, it is important to develop a model which contains the most distinctive features of the full-folding approach as well as a realistic account of explicit medium effects. Extensive work has been done in the past towards achieving this goal based on what is generally known as the *folding model* for the optical potential [7–10]. This model relies on a local density argument to obtain an effective internucleon force from infinite nuclear matter calculations. Further averaging procedures are devised to obtain a local effective force which depends on the density of the target nucleus as well as on the energy of the incident nucleon. Although quite successful in describing the scattering data, mainly in the 100–200 MeV region, the folding model treats indirectly the off-shell properties and the intrinsic energy dependence of the effective force. Furthermore, with the construction of such a simplified local effective interaction it becomes impossible to identify unambiguously the role and importance of effects due to the nuclear medium relative to genuine off-shell contributions.

Recently, some effort has been made [11,12] to improve the calculation of the optical potential starting from the NN t matrix. With the use of the $t\rho$ approximation for the leading term of the optical potential, medium effects have been introduced to second order when considering particle propagation in the finite target nucleus [11]. Al-

ternatively, a different approach has been followed [12] with corrections to the optical potential coming from binding energy and Pauli blocking effects. Whether these approaches will be successful in providing a systematic description of the data remains to be seen as they have only been applied to NA scattering above 80–100 MeV and to lighter targets ($A \leq 40$).

In this paper we develop a framework to account for medium effects in the calculation of the nonlocal and energy-dependent effective internucleon force and then generalize the full-folding model to include these effects in the calculation of the NA optical potential. Our approach to the calculation of the effective NN interaction provides a formalism which can be used as a starting point for simplifying schemes in subsequent calculations. For example, the idea of the local density approximation [7] for the optical potential can be derived as a limiting case of this more general approach.

In principle, the effective NN interaction depends on specific properties of the target nucleus and its excitation spectrum. However, most nucleon scattering data and the associated phenomenological analyses suggest that the NA optical potential depends primarily on gross properties of the target nuclei rather than on particular details [13]. Based on this fact, we use a global single-particle model based on infinite nuclear matter to describe the particle propagation in the nuclear medium rather than a target–specific model. Thus we incorporate average medium effects throughout the density of the target nucleus. The resulting effective force can be identified with the nuclear matter g matrix. Nevertheless, as will be shown, we do not need to invoke a local density argument to use this g matrix in the full-folding model.

This paper is organized as follows. In Sec. II we develop the formalism for constructing an effective two-nucleon interaction starting from the bare NN force. We discuss an approximate solution for the effective force and show how it can be calculated in the context of a given model for the target nucleus. Then in Sec. III we obtain a generalized expression for the full-folding model for the optical potential. In Sec. IV we show the results of our calculations for proton elastic scattering from ^{40}Ca and ^{208}Pb in the 30–400 MeV energy range followed by a discussion concerning the relative importance of Pauli blocking and the nuclear mean field in the scattering observables. In Sec. IV we also present and discuss total cross section calculations for neutron elastic scattering from ^{40}Ca, ^{90}Zr, and ^{208}Pb. In Sec. V we summarize our work.

II. THE EFFECTIVE INTERACTION

In this section we present a formalism for calculating the NN effective force which takes into account the nuclear medium. The problem of constructing an *in medium* effective interaction starting from the bare internucleon force is crucial for evaluating the NA optical potential. Also, it plays a central role when evaluating a diversity of microscopic processes involving two nucleon transitions from an initial to a final state.

Our approach assumes that only two-nucleon correlations are important in the nuclear medium while other nucleons propagate without interacting with the pair [14,15]. In this context, the most important point relates to the construction of a two-nucleon propagator which determines the characteristics of the effective force. Since this calculation is very difficult for a finite nucleus, we shall eventually introduce an interacting nuclear matter model to describe the nuclear excitation spectrum. Once the effective interaction is constructed we discuss in Sec. III the calculation of the NA optical potential in the full-folding framework.

Let us consider the simplest model for a general two-nucleon force $F(\omega)$ which accounts for multiple scattering of the nucleons to all orders in the ladder approximation [14,15]. Then, for an initial or starting energy ω, F satisfies the integral equation

$$F(\omega) = V + V\,\Lambda(\omega)\,F(\omega)\ , \tag{1}$$

where V corresponds to the bare NN potential and $\Lambda(\omega)$ is a two-body propagator for nucleons propagating in the intermediate states.

The calculation of $F(\omega)$ in Eq. (1) faces two main difficulties: one is technical and relates to solving the full integral equation in a given representation for the two-body system. The other difficulty relates to the construction of the two-body propagator $\Lambda(\omega)$ which should account for the excitation modes of the target nucleus and the restrictions imposed by the Pauli exclusion principle.

A. Approximate solution for the two-nucleon force

To address the first issue mentioned above we consider matrix elements of the F force in a momentum representation. Denoting the center-of-mass momentum (c.m.) of two interacting nucleons by $\vec{K}$ and the relative momentum of the pair by $\vec{\kappa}$, Eq. (1) yields

$$\left\langle \vec{K}\,';\vec{\kappa}\,'\,|F(\omega)|\,\vec{K};\vec{\kappa}\right\rangle = \delta(\vec{K}-\vec{K}\,')\,\langle\vec{\kappa}\,'\,|V|\,\vec{\kappa}\rangle + \int d\vec{q}\,d\vec{Q}\,d\vec{q}\,'\,d\vec{Q}\,'\,\left\langle \vec{K}\,';\vec{\kappa}\,'\,|V|\,\vec{Q}\,';\vec{q}\,'\right\rangle \left\langle \vec{Q}\,';\vec{q}\,'\,|\Lambda(\omega)|\,\vec{Q};\vec{q}\right\rangle \times\left\langle \vec{Q};\vec{q}\,|F(\omega)|\,\vec{K};\vec{\kappa}\right\rangle\ , \tag{2}$$

where we have assumed that the bare NN interaction V conserves the total momentum for the NN pair. In order to investigate alternative ways to calculate the F-matrix elements beyond the "straightforward" numerical solution of Eq. (2), we introduce the average c.m. momentum $\vec{P}$ and the change in the c.m. momentum $\vec{p}$ defined by

$$\vec{P} = \tfrac{1}{2}(\vec{K}+\vec{K}\,')\ , \tag{3a}$$

$$\vec{p} = \vec{K} - \vec{K}' \,. \tag{3b}$$

Then, Eq. (2) can be written as

$$\left\langle \vec{P} - \tfrac{1}{2}\vec{p}; \vec{\kappa}' \right| F(\omega) \left| \vec{P} + \tfrac{1}{2}\vec{p}; \vec{\kappa} \right\rangle = \delta(\vec{p}) \langle \vec{\kappa}' | V | \vec{\kappa} \rangle + \int d\vec{p}'\, d\vec{q}\, d\vec{q}' \langle \vec{\kappa}' | V | \vec{q}' \rangle \times \left\langle \vec{P} - \tfrac{1}{2}\vec{p}; \vec{q}' \right| \Lambda(\omega) \left| \vec{P} - \tfrac{1}{2}\vec{p} - \vec{p}'; \vec{q} \right\rangle \left\langle \vec{P} - \tfrac{1}{2}\vec{p} - \vec{p}'; \vec{q} \right| F(\omega) \left| \vec{P} + \tfrac{1}{2}\vec{p}; \vec{\kappa} \right\rangle , \tag{4}$$

where we have integrated over the δ function associated with the NN total momentum conservation in the integrand. Guided by the translational invariance characteristic of two nucleons interacting in free space or in infinite nuclear matter, it is convenient to express the two-body matrix elements of F in the general case in terms of its (partial) Fourier transform over the c.m. position variable,

$$\left\langle \vec{P} - \tfrac{1}{2}\vec{p}; \vec{\kappa}' \right| F(\omega) \left| \vec{P} + \tfrac{1}{2}\vec{p}; \vec{\kappa} \right\rangle = \frac{1}{(2\pi)^3} \int d\vec{R}\, e^{i\vec{R}\cdot\vec{P}} \left\langle \vec{\kappa}' \right| f_{[\vec{P};\vec{R}]}(\omega) \left| \vec{\kappa} \right\rangle \,. \tag{5}$$

The function $\langle \vec{\kappa}' | f_{[\vec{P};\vec{R}]}(\omega) | \vec{\kappa} \rangle$ will be identified as the matrix elements of a reduced two-body effective force $f_{[\vec{P};\vec{R}]}(\omega)$ evaluated at the average c.m. momentum $\vec{P}$ and localized at the coordinate $\vec{R}$ in the system. Similarly, we take the following representation for the two-body propagator $\Lambda(\omega)$ by Fourier transforming over the c.m. coordinate,

$$\left\langle \vec{P} + \tfrac{1}{2}\vec{p}; \vec{q}' \right| \Lambda(\omega) \left| \vec{P} - \tfrac{1}{2}\vec{p}; \vec{q} \right\rangle = \frac{1}{(2\pi)^3} \int d\vec{R}\, e^{-i\vec{R}\cdot\vec{p}} \left\langle \vec{q}' \right| \lambda_{[\vec{P};\vec{R}]}(\omega) \left| \vec{q} \right\rangle \,, \tag{6}$$

where $\lambda_{[\vec{P};\vec{R}]}(\omega)$ is the reduced two-body propagator acting at the coordinates $\vec{P}$ and $\vec{R}$, respectively, and may be expressed as

$$\left\langle \vec{q}' \right| \lambda_{[\vec{P};\vec{R}]}(\omega) \left| \vec{q} \right\rangle = \int d\vec{r}\, e^{-i\vec{r}\cdot\vec{P}} \left\langle \vec{R} + \tfrac{1}{2}\vec{r}; \vec{q}' \right| \Lambda(\omega) \left| \vec{R} - \tfrac{1}{2}\vec{r}; \vec{q} \right\rangle \,. \tag{7}$$

The matrix elements of the reduced two-body force f are now obtained directly. From Eq. (5) we have

$$\left\langle \vec{\kappa}' \right| f_{[\vec{P};\vec{R}]}(\omega) \left| \vec{\kappa} \right\rangle = \int d\vec{p}\, e^{-i\vec{p}\cdot\vec{R}} \left\langle \vec{P} - \tfrac{1}{2}\vec{p}; \vec{\kappa}' \right| F(\omega) \left| \vec{P} + \tfrac{1}{2}\vec{p}; \vec{\kappa} \right\rangle \,. \tag{8}$$

Combining Eqs. (2), (5), (6), and (8) we obtain the following integral equation for the f force

$$f_{[\vec{P};\vec{R}]}(\omega) = V + \frac{1}{(2\pi)^6} \int d\vec{p} d\vec{p}' d\vec{R}' d\vec{R}''\, V\, \lambda_{\left[\vec{P} - \frac{\vec{p}}{2} - \frac{\vec{p}'}{2}; \vec{R}'\right]}(\omega)\, e^{-i\vec{p}'\cdot(\vec{R}' - \vec{R}'')}\, e^{-i\vec{p}\cdot(\vec{R} - \vec{R}'')} f_{\left[\vec{P} - \frac{\vec{p}'}{2}; \vec{R}''\right]}(\omega) \,, \tag{9}$$

where, for simplicity, we have suppressed the dependence of the matrix elements on the relative coordinates. Making use of Eq. (7) we can recast the integral equation for f in a more symmetric form. We obtain,

$$f_{[\vec{P};\vec{R}]}(\omega) = V + \frac{1}{(2\pi)^6} \int d\vec{r}\, d\vec{r}'\, d\vec{p}\, d\vec{p}'\, V\, \lambda_{[\vec{P}+\vec{p};\vec{R}+\vec{r}]}(\omega)\, e^{i(\vec{r}'\cdot\vec{p} - \vec{p}'\cdot\vec{r})} f_{\left[\vec{P} - \frac{\vec{p}'}{2}; \vec{R} - \frac{\vec{r}'}{2}\right]}(\omega) \,. \tag{10}$$

This is an exact result for the reduced two-body effective force f. It should be stressed that, up to this point, no assumption about nuclear structure has been made other than that of assuming the generalized force F is two-body in nature and satisfies Eq. (1).

The main advantage of Eq. (10) for f is that it provides a framework for developing approximations to simplify the calculation of the effective NN force. Indeed, if we expand perturbatively the solution to Eq. (10) we have, to second order in the bare interaction V,

$$f_{[\vec{P};\vec{R}]}(\omega) = V + V\, \lambda_{[\vec{P};\vec{R}]}(\omega) V + \cdots \,. \tag{11}$$

We observe that the leading nontrivial term for the force evaluated at the coordinate $\vec{R}$ and momentum $\vec{P}$ involves the λ propagator localized at the same position $\vec{R}$ and average c.m. momentum $\vec{P}$. Therefore, it is reasonable to expect that the dominant contribution to the integrand in Eq. (10) comes from those matrix elements of the λ propagator centered around the $\vec{P}$ and $\vec{R}$ coordinates while the interacting pair propagates in the intermediate states throughout the nuclear medium.

An approximate solution to Eq. (10) can be sought if we expand the λ propagator around $\vec{P}$ and $\vec{R}$,

$$\lambda_{[\vec{P}+\vec{p};\vec{R}+\vec{r}]}(\omega) = \lambda_{[\vec{P};\vec{R}]}(\omega) + \cdots \,, \tag{12}$$

and keep only the first order term. Thus we obtain a solution which we identify as a generalized g matrix which satisfies a simplified integral equation,

$$g_{[\vec{P};\vec{R}]}(\omega) = V + V\ \lambda_{[\vec{P};\vec{R}]}(\omega)\ g_{[\vec{P};\vec{R}]}(\omega)\,. \qquad (13)$$

This g matrix is much easier to calculate than the exact f matrix in Eq. (10) and yet can be regarded as a substantially improved first approximation for the effective force, relative to approximations which ignore the nuclear medium.

In general, the scheme we propose provides a result for the two-body effective force which enters in the calculation of the nuclear dynamics. As suggested by Eq. (5) we account very naturally for the c.m. motion of the interacting pair through a localization of the reduced two-body f force in the nuclear medium. Then, in the g-matrix approximation, the two-body F-matrix solution to Eq. (1) is

$$\left\langle \vec{P} - \tfrac{1}{2}\vec{p};\vec{\kappa}' \right| F(\omega) \left| \vec{P} + \tfrac{1}{2}\vec{p};\vec{\kappa} \right\rangle$$

$$\approx \frac{1}{(2\pi)^3}\int d\vec{R}\, e^{i\vec{R}\cdot\vec{p}} \left\langle \vec{\kappa}' \right| g_{[\vec{P};\vec{R}]}(\omega) \left| \vec{\kappa} \right\rangle . \qquad (14)$$

This new structure for the effective force will be applied later in this paper to the calculation of the nucleon-nucleus optical potential.

B. The two-body propagators

As mentioned previously, the other important issue related to the calculation of an effective force is the specification and construction of a propagator which describes adequately the propagation of the nucleon pair in the intermediate states. This consideration enters explicitly in the calculation of either the f matrix in Eq. (10) or the approximate g matrix in Eq. (13).

Quite generally, the reduced two-body λ propagator is obtained from the two-body Λ propagator through Eq. (7). On the other hand, the Λ propagator in a many-body system can be expressed as [15]

$$\langle \vec{q}_1\,';\vec{q}_2\,' \mid \Lambda(\omega) \mid \vec{q}_1;\vec{q}_2 \rangle = \int \frac{A(\vec{q}_1\,',\vec{q}_1;z)A(\vec{q}_2\,',\vec{q}_2;z')}{\omega - z - z' + i\eta} dz\, dz' , \qquad (15)$$

where $A(z)$ is the single-nucleon spectral function [15] and $\vec{q}_i$ are the single-particle momenta. The alternative models one might choose to describe the nuclear excitation spectrum determine the properties of the spectral function $A(z)$ and, therefore, of the two-body propagator.

In this work, we consider a symmetric, interacting Fermi gas for constructing the spectral function $A(z)$. Furthermore, we neglect hole propagation in the two-body propagator, an assumption usually adopted in the calculation of effective forces for nucleon scattering [16,17]. In a coordinate representation, the particle spectral function $A_p(z)$ for a Fermi gas characterized by a Fermi momentum k_F and a Fermi energy ϵ_F is given in a quasiparticle approximation by

$$A_p(\vec{x}\,',\vec{x};z) = \frac{1}{(2\pi)^3}\int d\vec{k}_\alpha \delta[z - \epsilon(k_\alpha;k_F)]\, e^{i\vec{k}_\alpha\cdot(\vec{x}\,'-\vec{x})} \times\Theta[\epsilon(k_\alpha;k_F) - \epsilon_F]\,. \qquad (16)$$

Here, $\epsilon(k_\alpha;k_F)$ is the single-particle energy of a nucleon of momentum k_α in the infinite medium of Fermi momentum k_F [16],

$$\epsilon(k_\alpha;k_F) = \frac{k_\alpha^2}{2m} + \mathrm{Re}\,[U_{\mathrm{NM}}(k_\alpha;k_F)]\ , \qquad (17)$$

with m the nucleon mass, $\hbar = 1$ and $U_{\mathrm{NM}}(k_\alpha;k_F)$ the complex self-consistent mean field at k_F. The problem arises as to how the nuclear matter particle spectral function may be related to the corresponding spectral function of a finite system. We adopt the widely used prescription

$$\rho(R) = \frac{2}{3\pi^2}k_F^3(R)\,, \qquad (18)$$

to relate the density ρ of the nucleus with that of the Fermi gas, thus generating a spatial dependence for k_F as we identify $\vec{R}$ with the average coordinate of the interacting nucleons,

$$\vec{R} = \tfrac{1}{2}(\vec{x} + \vec{x}\,')\,. \qquad (19)$$

Now we can calculate the particle spectral function in momentum space for further use in Eq. (15) for the two-body propagator $\Lambda(\omega)$. From Eq. (16) and using the prescription expressed by Eqs. (16)–(19) we have in momentum space

$$A_p(\vec{q}_1\,',\vec{q}_1;z) = \frac{1}{(2\pi)^3}\int d\vec{r}\, d\vec{R}\, e^{i\vec{R}\cdot(\vec{q}_1-\vec{q}_1\,')}\, e^{i\vec{r}\cdot\left(\frac{\vec{q}_1+\vec{q}_1\,'}{2}\right)} \times A_p(\vec{R} - \tfrac{1}{2}\vec{r},\vec{R} + \tfrac{1}{2}\vec{r};z)\,, \qquad (20)$$

where $\vec{r} = \vec{x} - \vec{x}\,'$. Introducing the average and transferred momenta,

$$\vec{P}_1 = \tfrac{1}{2}(\vec{q}_1 + \vec{q}_1\,')\,, \qquad (21a)$$

$$\vec{p}_1 = \vec{q}_1 - \vec{q}_1\,', \qquad (21b)$$

and integrating over the relative coordinate $\vec{r}$ we obtain for the particle spectral function

$$A_p(\vec{P}_1 - \tfrac{1}{2}\vec{p}_1,\vec{P}_1 + \tfrac{1}{2}\vec{p}_1;z) = A_p(\vec{P}_1,\vec{p}_1;z) = \frac{1}{(2\pi)^3}\int d\vec{R}\, e^{i\vec{R}\cdot\vec{p}_1}\, \delta[z - \epsilon(P_1;k_F(R))]\, \Theta[\epsilon(P_1;k_F(R)) - \epsilon_F(R)]\,. \qquad (22)$$

The calculation of the two-body Λ propagator is now straightforward. Introducing Eq. (22) for the particle spectral function in Eq. (15) for the two-nucleon propagator, and neglecting the delocalization of the two particles in the

medium when integrating over the spatial coordinates,

$$k_F\left(\left|\vec{R}\pm\tfrac{1}{2}\vec{r}\right|\right)\approx k_F(R)\,, \tag{23}$$

we obtain for the Λ propagator, expressed in the c.m. ($\vec{Q}$) and relative momentum ($\vec{q}$) coordinates for the nucleon pair [Eq. (2)],

$$\left\langle \vec{Q}';\vec{q}' \mid \Lambda(\omega) \mid \vec{Q};\vec{q}\right\rangle = \delta[\vec{q}-\vec{q}'\,]\times\tilde{\Lambda}\left(\tfrac{1}{2}(\vec{Q}+\vec{Q}');(\vec{Q}-\vec{Q}');\vec{q};\omega\right), \tag{24}$$

with

$$\tilde{\Lambda}\left(\tfrac{1}{2}(\vec{Q}+\vec{Q}');(\vec{Q}-\vec{Q}');\vec{q};\omega\right)=\frac{1}{(2\pi)^3}\int d\vec{R}\,e^{i\vec{R}\cdot(\vec{Q}-\vec{Q}')}\,\lambda^{\rm NM}_{\frac{1}{2}(\vec{Q}+\vec{Q}')}(\vec{q};\omega;k_F(R))\,, \tag{25}$$

and $\lambda^{\rm NM}$ is the nuclear matter single-particle propagator [16] at the Fermi momentum k_F

$$\lambda^{\rm NM}_{\vec{p}}(\vec{q}\,;\,\omega\,;\,k_F)=\frac{\mathcal{Q}(P_+\,;P_-\,;k_F\,)}{\omega+i\eta-\epsilon(P_+;k_F)-\epsilon(P_-;k_F)}\,, \tag{26}$$

with $P_\pm=\left|\frac{1}{2}\vec{P}\pm\vec{q}\right|$ and $\mathcal{Q}$ the Pauli blocking function

$$\mathcal{Q}(P_+\,;P_-\,;k_F\,)=\Theta[\,\epsilon(P_+;k_F)-\epsilon_F\,]\times\Theta[\,\epsilon(P_-;k_F)-\epsilon_F\,]\,. \tag{27}$$

Equations (24)–(26) for $\Lambda(\omega)$ represent a particular two-body propagator for nucleons in a finite nucleus. The interacting Fermi gas used to calculate this propagator averages the effect of the gas throughout the nucleus via the local density ansatz used to construct the single-particle spectral function in Eq. (22). We remark, however, that the local density ansatz expressed by Eqs. (16)–(19) need not be used as a means of modeling the two-body propagator in a finite nucleus and therefore for calculating the effective force F. Other more realistic models could be used to account for this effect. In this sense the present approach is general and departs notably from more intuitive ways used to define an effective force [7–10].

The reduced λ propagator required to calculate either the f or the g matrix, Eq. (10) or (13), respectively, is obtained directly from Eqs. (7) and (24),

$$\left\langle \vec{q}'\,\middle|\,\lambda_{[\,\vec{P}\,;\,\vec{R}\,]}(\omega)\,\middle|\,\vec{q}\right\rangle=\delta[\vec{q}-\vec{q}'\,]\,\lambda^{\rm NM}_{\vec{p}}(\vec{q};\omega;k_F(R))\,. \tag{28}$$

This result completes our scheme for calculating the internucleon effective force F which, in the g-matrix approximation, is given by Eq. (14). It is interesting to note that although we use a local density ansatz to construct the single-particle spectral function in the quasiparticle approximation, the resulting effective force F only displays a functional dependence on the density of the target nucleus. Indeed, the density only enters in determining the radial ($\vec{R}$) dependence of the g matrix in Eq. (13).

III. THE OPTICAL POTENTIAL

In this work we focus on investigating the role of medium effects in the leading term of the optical potential. The NA optical potential for a nucleon of energy E can be cast, in momentum space, as the antisymmetrized matrix elements of the NN effective interaction F [1–4,14,18,19],

$$U(\vec{k}\,',\vec{k};E)=\sum_{\alpha\le\epsilon_F}\left\langle\vec{k}\,';\phi_\alpha\,|F(E+\epsilon_\alpha)|\,\vec{k};\phi_\alpha\right\rangle_A\,, \tag{29}$$

with $\{\phi_\alpha,\epsilon_\alpha\}$ the single-particle wave functions and energies of the target ground state; $\vec{k}$ and $\vec{k}\,'$ are momenta associated with the scattered nucleon. Using the two-body force $F(\omega)$, as expressed in Eq. (5), we obtain

$$U(\vec{k}\,',\vec{k};E)=\frac{1}{(2\pi)^3}\sum_{\alpha\le\epsilon_F}\int d\vec{R}\,d\vec{P}\,d\vec{p}\,e^{i\vec{R}\cdot(\vec{q}-\vec{p})}\rho_\alpha(\vec{P}+\tfrac{1}{2}\vec{p},\vec{P}-\tfrac{1}{2}\vec{p})\times\left\langle\vec{\kappa}\,'-\tfrac{1}{4}(\vec{p}-\vec{q})\,\middle|\,f_{[\,\vec{R}+\vec{P}\,;\,\vec{R}\,]}(E+\epsilon_\alpha)\,\middle|\,\vec{\kappa}+\tfrac{1}{4}(\vec{p}-\vec{q})\right\rangle_A\,, \tag{30}$$

where we have denoted

$$\vec{\kappa}\,'=\tfrac{1}{2}(\vec{K}-\vec{P}-\vec{q})\,,\quad \vec{\kappa}=\tfrac{1}{2}(\vec{K}-\vec{P}+\vec{q})\,, \tag{31}$$

with $\vec{K}$ and $\vec{q}$ defined by

$$\vec{K}=\tfrac{1}{2}\,(\vec{k}+\vec{k}\,')\,, \tag{32a}$$

$$\vec{q}=\vec{k}-\vec{k}\,'\,, \tag{32b}$$

corresponding to the average and transferred momentum of the projectile, respectively; the ground state density ρ_α associated with the state α is given by

$$\rho_\alpha(\vec{P}+\tfrac{1}{2}\vec{p},\vec{P}-\tfrac{1}{2}\vec{p})=n_\alpha\,\phi^\dagger_\alpha(\vec{P}+\tfrac{1}{2}\vec{p})\phi_\alpha(\vec{P}-\tfrac{1}{2}\vec{p})\,, \tag{33}$$

with n_α the occupancy of level α.

Equation (30) represents the most general expression for the leading term of the optical potential when the effective interaction is calculated taking into account finite

size effects. An advantage of this approach over now standard finite nucleus models [7,9] is that we do not require an explicit local density assumption to convolute the effective force with the target density. Furthermore, we are able to keep track of the approximations that need to be introduced when establishing the connection between the finite many-body problem and the construction of an effective force which incorporates nuclear correlations in a realistic way.

The calculation of the optical potential as expressed by Eq. (30) is quite challenging. It involves the calculation of the reduced force f from Eq. (10) and the evaluation of multidimensional integrals. In order to find an approximate, simplified expression for the optical potential, let us introduce the Wigner transform [17] W_α of the single-particle density ρ_α, namely

$$W_\alpha(\vec{R};\vec{P}) = \frac{1}{(2\pi)^3}\int d\vec{p}\, e^{-i\vec{R}\cdot\vec{p}}\,\rho_\alpha(\vec{P}+\tfrac{1}{2}\vec{p},\vec{P}-\tfrac{1}{2}\vec{p})\,. \tag{34}$$

Then, replacing Eq. (34) in Eq. (30) and making the change of variable $\vec{p}\to\vec{p}+\vec{q}$, we obtain

$$U(\vec{k}\,',\vec{k};E) = \frac{1}{(2\pi)^3}\sum_\alpha \int d\vec{R}d\vec{R}\,'d\vec{P}d\vec{p}\, e^{i\vec{R}\,'\cdot\vec{q}}W_\alpha(\vec{R}\,';\vec{P})\, e^{i\vec{p}\cdot(\vec{R}\,'-\vec{R})} \times\left\langle \vec{\kappa}\,' - \tfrac{1}{4}\vec{p}\,\middle|\, f_{[\vec{K}+\vec{P};\vec{R}]}(E+\epsilon_\alpha)\,\middle|\,\vec{\kappa}+\tfrac{1}{4}\vec{p}\right\rangle_A . \tag{35}$$

Now we realize that the role of the momentum $\vec{p}$ in Eq. (35) is to give a measure of the delocalization of the average bound nucleon ($\vec{R}\,'$) with respect to the average incoming particle ($\vec{R}$). Since the f-matrix elements do not depend on $\vec{p}$ for an $\vec{R}$ independent interaction f, we have assumed in the general case that a weak dependence on $\vec{p}$ justifies taking $\vec{p}=0$ when evaluating the f-matrix elements in the integrand of Eq. (35). We expect this approximation to be reasonable since the off-shell sampling is still dominated by the variation of the average momentum $\vec{P}$ of the target nucleons. Thus, the optical potential becomes

$$U(\vec{k}\,',\vec{k};E) \simeq \int d\vec{R}\, e^{i\vec{q}\cdot\vec{R}}\sum_\alpha\int d\vec{P}\, W_\alpha(\vec{R};\vec{P}) \times\left\langle \vec{\kappa}\,'\,\middle|\, f_{[\vec{K}+\vec{P};\vec{R}]}(E+\epsilon_\alpha)\,\middle|\,\vec{\kappa}\right\rangle_A . \tag{36}$$

Equation (36) is an explicit expression for the optical potential in terms of the local nuclear density in phase space (W_α) and the reduced effective force acting between the interacting nucleons at each $\vec{R}$ coordinate in the system. When the f matrix is approximated by the g matrix and the latter is calculated using nuclear matter correlations for the propagator in the intermediate states [Eq. (28)], then Eqs. (35) and (36) for U provide a framework for developing the local density (and other) approximations. In this way, our derivation overcomes some of the heuristic arguments often used to relate nuclear matter and finite nucleus results.

In the limit of a medium independent internucleon interaction, as in the case when using the free NN t matrix as the effective interaction, we recover the expression for the full-folding optical potential used in some of our earlier work [4,20], namely $U(\vec{k}\,',\vec{k};E)\to U_o(\vec{k}\,',\vec{k};E)$, with

$$U_o(\vec{k}\,',\vec{k};E) = \sum_\alpha\int d\vec{P}\,\rho_\alpha(\vec{P}+\tfrac{1}{2}\vec{q},\vec{P}-\tfrac{1}{2}\vec{q}) \times\left\langle \vec{\kappa}\,'\,\middle|\, t_{[\vec{K}+\vec{P}]}(E+\epsilon_\alpha)\,\middle|\,\vec{\kappa}\right\rangle_A . \tag{37}$$

The results presented later in this work use the g matrix as the effective interaction instead of the exact f matrix. Moreover, we introduce two further simplifications which we estimate shall not change our findings significantly. One simplification refers to taking an average binding energy $\bar{\epsilon}$ for each single-particle state of the bound nucleons [20]. In this case, Eq. (36) reduces to

$$U(\vec{k}\,',\vec{k};E) = \int d\vec{R}\int d\vec{P}\, e^{i\vec{q}\cdot\vec{R}}\, W(\vec{R};\vec{P}) \times\left\langle \vec{\kappa}\,'\,\middle|\, g_{[\vec{K}+\vec{P};\vec{R}]}(E+\bar{\epsilon})\,\middle|\,\vec{\kappa}\right\rangle_A , \tag{38}$$

with $W(\vec{R};\vec{P})$ the Wigner transform of the target mixed density,

$$W(\vec{R};\vec{P}) = \sum_\alpha W_\alpha(\vec{R};\vec{P}) = \frac{1}{(2\pi)^3}\int d\vec{p}\, e^{-i\vec{R}\cdot\vec{p}}\rho(\vec{P}+\tfrac{1}{2}\vec{p},\vec{P}-\tfrac{1}{2}\vec{p})\,. \tag{39}$$

The other simplification refers to using an approximate form for the mixed density [20,21], namely

$$\rho(\vec{P}+\tfrac{1}{2}\vec{p},\vec{P}-\tfrac{1}{2}\vec{p}) \approx \rho(p;P) = \frac{4}{(2\pi)^3}\int d\vec{R}\rho(R)e^{i\vec{p}\cdot\vec{R}}\frac{1}{\hat{\rho}(R)} \times\Theta[\hat{k}(R)-P]\,, \tag{40}$$

with $\hat{k}(R)$ a local momentum function given by either the Slater or Campi-Bouyssy approximations [21], and

$$\hat{\rho}(R) = \frac{2}{3\pi^3}\hat{k}_F^3(R). \tag{41}$$

In this case the Wigner transform takes a simple form given by

$$W(\vec{R};\vec{P}) = \frac{4}{(2\pi)^3}\rho(R)\,\frac{1}{\hat{\rho}(R)}\,\Theta[\hat{k}(R)-P]\,, \tag{42}$$

with ρ the target ground state density. Using this result in Eq. (38) we obtain an explicit expression for the optical potential in the g-matrix approximation,

$$U(\vec{k}',\vec{k};E)=\frac{4}{(2\pi)^3}\int d\vec{R}\,e^{i\vec{q}\cdot\vec{R}}\rho(R)\left\{\frac{1}{\hat{\rho}(R)}\int d\vec{P}\,\Theta[\hat{k}(R)-P]\left\langle\vec{\kappa}'\left|g_{[\vec{K}+\vec{P}\,;\,\vec{R}]}(E+\bar{\epsilon})\right|\vec{\kappa}\right\rangle_A\right\}. \tag{43}$$

In actual calculations Eq. (43) separates into proton and neutron contributions. For example, for proton scattering we have the schematic form $U\sim\rho_p g^{pp}+\rho_n g^{pn}$.

It is interesting to note from Eq. (43) how the approximate mixed density naturally suggests a nuclear matter approach for calculating the effective force. This is made explicit with the introduction of the Wigner transform which provides a representation where at each point $\vec{R}$ in the nucleus the momentum of the target nucleons is uniformly distributed up to a value $\hat{k}(R)$. Indeed, in the Slater prescription for the local momentum function we have $\hat{k}(R)=k_F(R)$, with the Fermi momentum k_F given in terms of the local density ρ by Eq. (18). Then, at each point $\vec{R}$ in the nucleus the Pauli blocking forces the interacting nucleons to propagate, on average, with momenta above $k_F(R)$ in the intermediate states and generates a particular $\vec{R}$ dependence for the effective force. However, as it has been stressed earlier, the $\vec{R}$ dependence of the force could be determined in more detail for each target provided a more realistic model is used to calculate the particle spectral functions (Eq. 15) leading to the construction of the reduced λ propagator in Eq. (7).

A final point remains to be clarified regarding the choice of the average energy $\bar{\epsilon}$ of the nucleons in the target. Following the nuclear matter model used in constructing the two-nucleon propagator Λ [Eqs. (24)–(27)] which determines the effective interaction, we consider the most consistent definition for the nucleon average binding energy to be

$$\bar{\epsilon}\to\bar{\epsilon}(R)=\frac{\sum_\alpha\Theta[k_F(R)-k_\alpha]\epsilon(k_\alpha;k_F(R))}{\sum_\alpha\Theta[k_F(R)-k_\alpha]}, \tag{44}$$

with $\epsilon(k_\alpha;k_F)$ the single-particle energy in nuclear matter given by Eq. (6). An alternative approach is to calculate $\bar{\epsilon}$ from realistic single-particle energies in the target nucleus [20], but we find that the different prescriptions make no major differences in the calculated observables as will be discussed in the next section.

IV. RESULTS

In this section we report results obtained from the theory developed in Secs. II and III. The full-folding optical potentials given by Eq. (43) were calculated following the general procedure outlined elsewhere [4]. The effective internucleon force, the g matrix, was calculated using correlations obtained from infinite nuclear matter. Applications have been made for proton elastic scattering on ^{40}Ca and ^{208}Pb in the 30–400 MeV energy range. By considering two targets of very different size we expect to have a stringent test on the theory. Also, we have included calculations of total cross sections for neutron scattering from different targets.

A. Calculation of the effective interaction

The two-body effective interaction for the NN pair can be expressed in terms of a reduced effective force as shown in Eq. (5) or (14) which reduces the problem to calculating either the f or g matrix depending on the level of approximations introduced in the two-body Λ propagator. In the context of Sec. II, where we use symmetric nuclear matter information to construct the reduced λ propagator (Eq. 28), the g matrix as expressed by Eq. (13) satisfies a Bethe-Goldstone integral equation [16],

$$\begin{aligned}\left\langle\vec{\kappa}'\left|g_{[\vec{P}\,;\,\vec{R}]}(\omega)\right|\vec{\kappa}\right\rangle &= \langle\vec{\kappa}'\,|V|\,\vec{\kappa}\rangle+\int d\vec{\kappa}''\,\langle\vec{\kappa}'\,|V|\,\vec{\kappa}''\rangle\\ &\times\lambda^{\rm NM}_{\vec{P}}(\vec{\kappa}'';\omega;k_F(R))\\ &\times\left\langle\vec{\kappa}''\left|g_{[\vec{P}\,;\,\vec{R}]}(\omega)\right|\vec{\kappa}\right\rangle,\end{aligned} \tag{45}$$

with $\lambda^{\rm NM}$ defined by Eq. (26) and the $\vec{R}$ dependence specified through the relationship between the target density ρ and the Fermi momentum k_F in Eq. (18).

The g matrix was calculated using the Paris [22] potential V by solving the integral equation [Eq. (45)] using standard matrix inversion methods [23]. Both central and spin-orbit parts of the g matrix were used to calculate the NA optical potential. The $\vec{R}$ dependence was obtained by calculating the g matrix at different densities corresponding to k_F values in the 0–1.4 fm^{-1} range. The real mean field, $U_{\rm NM}(k;\,k_F)$ in Eq. (17), was determined self-consistently from

$$\begin{aligned}U_{\rm NM}(k;\,k_F)=\sum_{\alpha\le\epsilon_F}&\left\langle\tfrac{1}{2}(\vec{k}-\vec{k}_\alpha)\left|g_{[\vec{k}+\vec{k}_\alpha]}(\epsilon(k)+\epsilon(k_\alpha))\right.\right.\\ &\times\left.\left|\tfrac{1}{2}(\vec{k}-\vec{k}_\alpha)\right\rangle\right.,\end{aligned} \tag{46}$$

using the continuous prescription [16] for Re$[U_{\rm NM}]$ at the Fermi energy. The Pauli blocking effect represented by Q in Eq. (26) was simplified to its angle-averaged form. Since we emphasize an accurate off-shell sampling of the NN effective interaction, the g matrix was calculated at several (over 16) values of the total NN c.m. momentum in the 0 – 7 fm^{-1} interval. Higher densities of mesh points were used in regions where the g matrix, as a function of the NN c.m. momentum, varies most rapidly.

In Figs. 1 and 2 we show, for reference, the results of symmetric nuclear matter calculations we have performed for the mean field $U_{\rm NM}$. In Fig. 1 we present the real part of $U_{\rm NM}$ as a function of the momentum k for several values of k_F. In Fig. 2 we show the corresponding imaginary part of $U_{\rm NM}$. Our results for the Paris potential agree with other similar calculations [24,25].

Another consideration in the present calculations was the treatment of the deuteron singularity in both the g and the t matrix. As discussed recently [5], a correct cal-

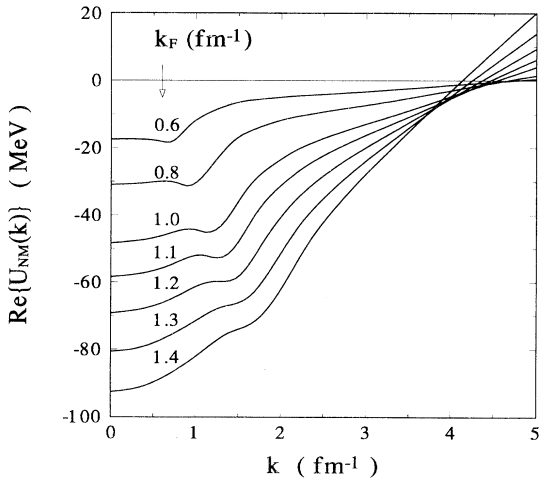

FIG. 1. Real part of the self-consistent mass operator in nuclear matter for k_F between 0.6 and 1.4 fm^{-1}.

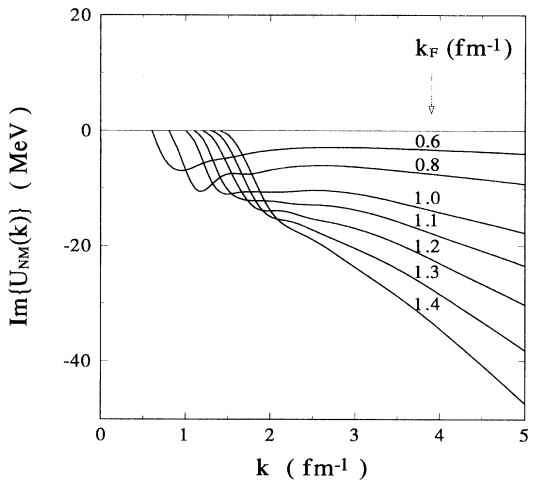

FIG. 2. Imaginary part of the self-consistent mass operator in nuclear matter for k_F between 0.6 and 1.4 fm^{-1}.

culation of the NN interaction off-shell as required by full-folding calculations samples regions in phase space near the deuteron bound state. In this region the effective force varies rapidly as a function of the total momentum of the interacting pair. Although this aspect was addressed in the context of the free t matrix, similar features are observed in the case of the g matrix for finite (nonzero) density. The effects in the case of the g matrix are less pronounced than in the t matrix case, with the pole singularity following a trend similar to that reported in studies of the propagation of deuterons in nuclear matter [26]. We have adapted our computing codes in order to evaluate deuteron contributions in the calculation of the optical potential [5].

B. Proton elastic scattering

Applications were made for elastic scattering of protons on ^{40}Ca and ^{208}Pb. The nuclear density for ^{40}Ca was determined from a single-particle model using a Woods-Saxon parametrization for the mean field to fit the rms radius of the point-proton density determined from electron scattering and to experimental single-particle energies [20]. The average single-particle energy $\bar{\epsilon}$ for protons and neutrons ($\bar{\epsilon}_p$ and $\bar{\epsilon}_n$) was estimated from the interacting Fermi gas for consistency following Eq. (44). Then we have that $\bar{\epsilon}_p$ and $\bar{\epsilon}_n$ vary inside the nucleus, as a function of the radial dependence of the corresponding density distributions. For comparison, we find $\bar{\epsilon}_p = -24.0$ MeV and $\bar{\epsilon}_n = -31.4$ MeV in the Woods-Saxon model. The overall average binding is $\bar{\epsilon} = \frac{1}{A}(Z\bar{\epsilon_p} + N\bar{\epsilon_n}) = -27.7$ MeV, with Z the proton number, N the neutron number, and $A = Z + N$. Although the values for the average nucleon binding vary significantly according to the model used, it is worthwhile to remark that on average the nucleus has a typical Fermi momentum in the range 0.8 – 1.0 fm^{-1}. Therefore, the dominant contributions to the g matrix come with an average nucleon binding in the range of -22 to -32 MeV which is close to the realistic average value of -27.7 MeV obtained from the single-particle model. In the case of ^{208}Pb the nuclear density was determined from the work by Negele [27] which gives an overall average binding $\bar{\epsilon} = -24.0$ MeV. However, in our calculations we followed the binding energy procedure outlined in the ^{40}Ca case since the same considerations apply. For calculations where no medium corrections are included and the t matrix acts as the effective NN force, we have used the average nucleon binding given by the realistic single-particle model throughout.

Calculations of differential cross sections ($d\sigma/d\Omega$), analyzing powers (A_y), and spin rotation functions (Q) were made for proton elastic scattering on ^{40}Ca and ^{208}Pb at energies between 30 and 400 MeV. Coulomb scattering was treated as described elsewhere [4].

In Figs. 3–5 we present calculations for p+^{40}Ca elastic scattering and compare them to the measured observables at 30.3 [28,29], 40 [30,31], 65 [32], 80 [33,34], 160 [33,34], 181 [34,35], 200 [36], 300 [37,38], and 400 [37] MeV as functions of the momentum transfer. The full curves represent our most complete full-folding calculations using the nuclear matter g matrix for the NN effective force. The dashed curves represent calculations based on the free t matrix. We note that medium effects are present throughout the range of energies considered in this analysis, as evidenced by differences between scattering observables obtained using g- and t-matrix approaches. These differences are more evident at energies of 200 MeV and below, particularly in the cross sections. We also note that the medium corrected full-folding calculations (solid curves) provide a systematic and qualitatively correct description of the data. Difficulties do appear, however, in describing the spin observables with the g-matrix approach, especially in the lower energy regime. We have explored possible sources of sensitivity of our results such as density, prescription for $\hat{k}(R)$ in Eq. (41), average binding energies, and deuteron contributions and

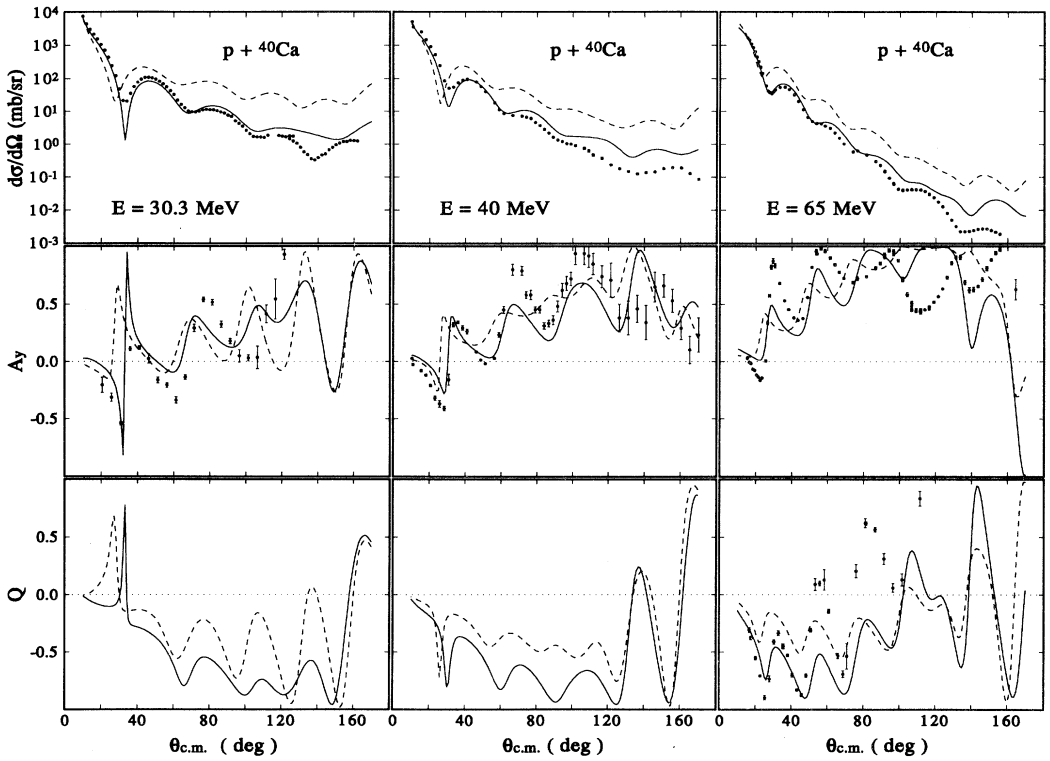

FIG. 3. Measured and calculated observables for p+^{40}Ca elastic scattering at 30.3, 40, and 65 MeV. The solid curves represent results from g-matrix full-folding calculations as described in the text. The dashed curves correspond to full-folding calculations using the free t matrix. See text for references to the data.

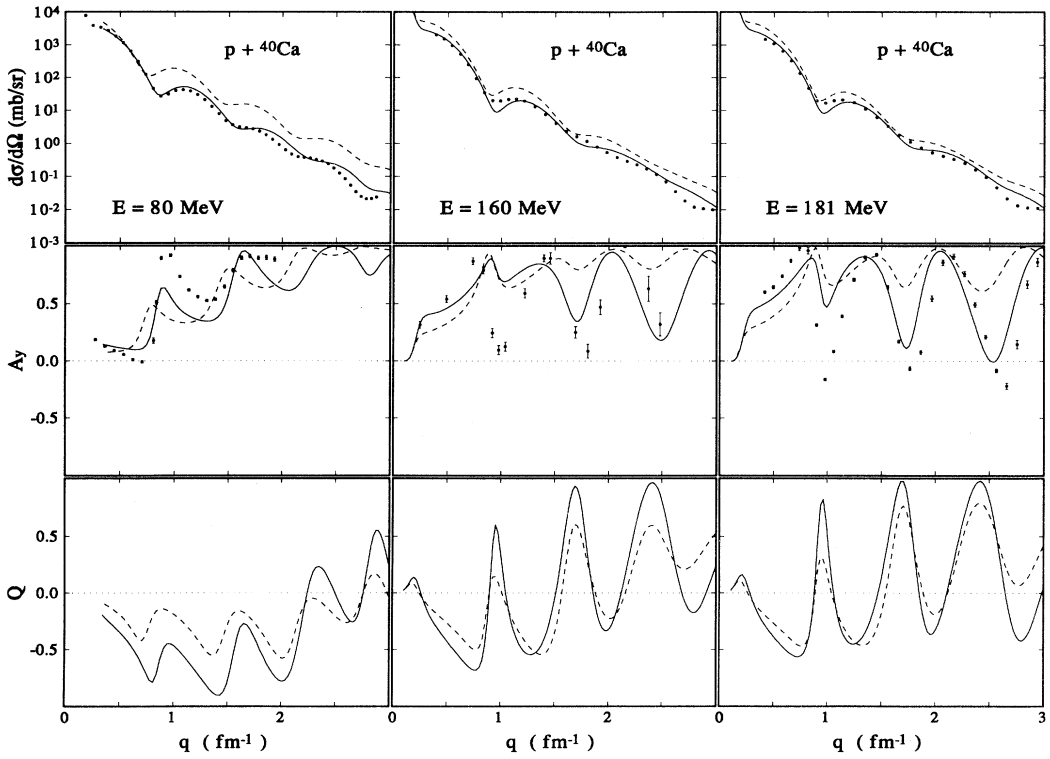

FIG. 4. As in Fig. 3 for p+^{40}Ca elastic scattering at 80, 160, and 181 MeV.

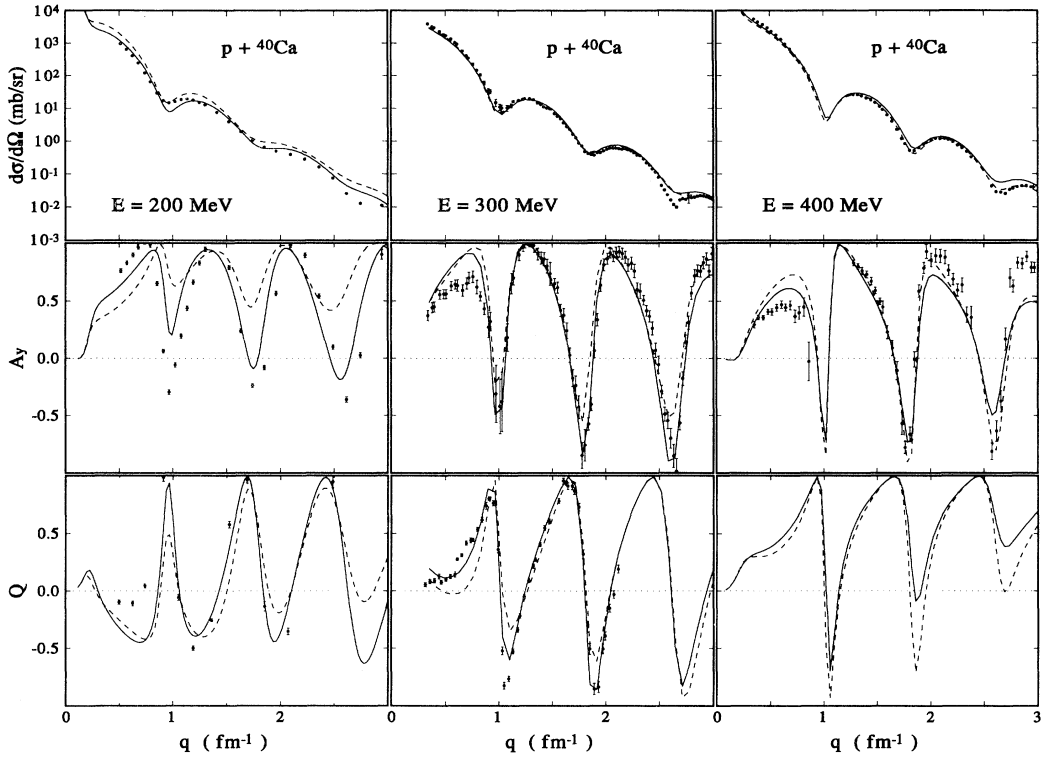

FIG. 5. As in Fig. 3 for p+^{40}Ca elastic scattering at 200, 300, and 400 MeV.

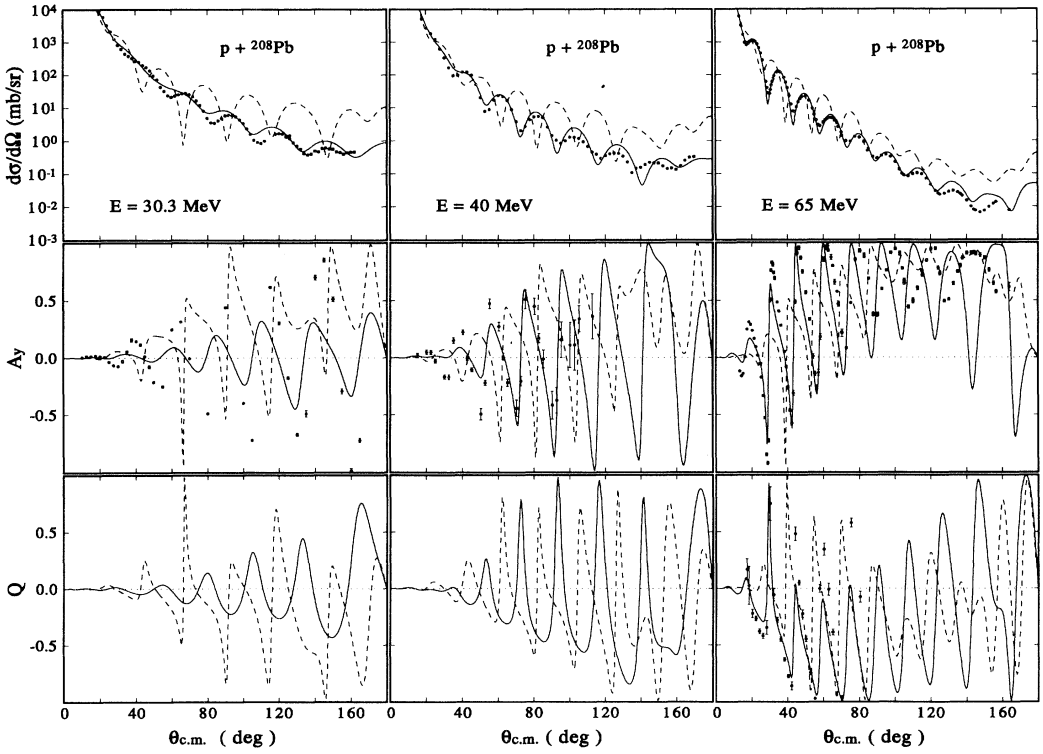

FIG. 6. As in Fig. 3 for p+^{208}Pb elastic scattering at 30.3, 40, and 65 MeV.

find variations much too small to account for differences between the theory and experiment.

In Figs. 6–8 we present calculations for p+^{208}Pb elastic scattering corresponding to measured observables at energies of 30.3 [28,29], 40 [39], 65 [32], 80 [34,33], 98 [34], 160 [33], 200 [37], 300, [37], and 400 [37] MeV. As in the previous case, the full curves correspond to results based on the g-matrix approach for the NN effective interaction and the dashed curves correspond to those based on the free t matrix. Overall, the theory works better for this heavier nucleus than for ^{40}Ca. This result is consistent with the hypothesis used in calculating the effective NN interaction. Furthermore, the agreement between the full-folding model and the data at energies between 65 and 400 MeV is remarkable when using the g matrix. At 400 MeV, however, the description of the analyzing power deteriorates, and the differential cross section is overestimated at $q > 1$ fm^{-1}. At 30.3 MeV we still have a quite reasonable description of the differential cross section, but the analyzing power is poorly reproduced. Another interesting result is that differences between g- and t-matrix approaches are quite evident throughout the energy range considered, a feature already noted in the case of p+^{40}Ca scattering. These differences are very pronounced at energies of 200 MeV and below.

The results for proton elastic scattering on ^{40}Ca and ^{208}Pb shown in Figs. 3–8 represent the most complete test of a parameter free approach to the optical potential over a wide range of energies. Although the present calculations show some improvement over the early folding models with density-dependent effective forces [7,9,10], it is clear that more work needs to be done in order to describe more accurately the data below 200 MeV. The average correlations provided by nuclear matter and used to construct the effective force do not appear detailed enough to allow the calculation of a sufficiently realistic g matrix at these lower energies. These findings are less optimistic than results reported recently [11] for proton scattering based on a $t\rho$ approach to the optical potential.

Regardless of the overall quality of our description of the data in the 30–400 MeV range, we are able to clarify some points concerning the role of the nuclear medium in determining the scattering observables in the intermediate energy region. At 400 MeV beam energy we observe that medium effects become more visible than would have been expected from the converging trend observed between the g- and t-matrix approaches at lower energies. Indeed, scattering results for both ^{40}Ca and ^{208}Pb at 300 MeV show relatively small differences between the g and t matrix approaches. At 400 MeV, however, we note an increase in the differences between the two approaches, particularly for ^{208}Pb, which supports the fact that medium effects are still relevant at these energies. These differences are due to the nature of the physical content of the NN effective force. The free t-matrix propagator does not account for Pauli blocking nor nuclear mean fields.

In order to understand better the role of Pauli blocking and the nuclear mean fields in nucleon scattering, we have calculated the cross sections and analyzing powers corresponding to p+^{208}Pb scattering at 98, 200, and 400

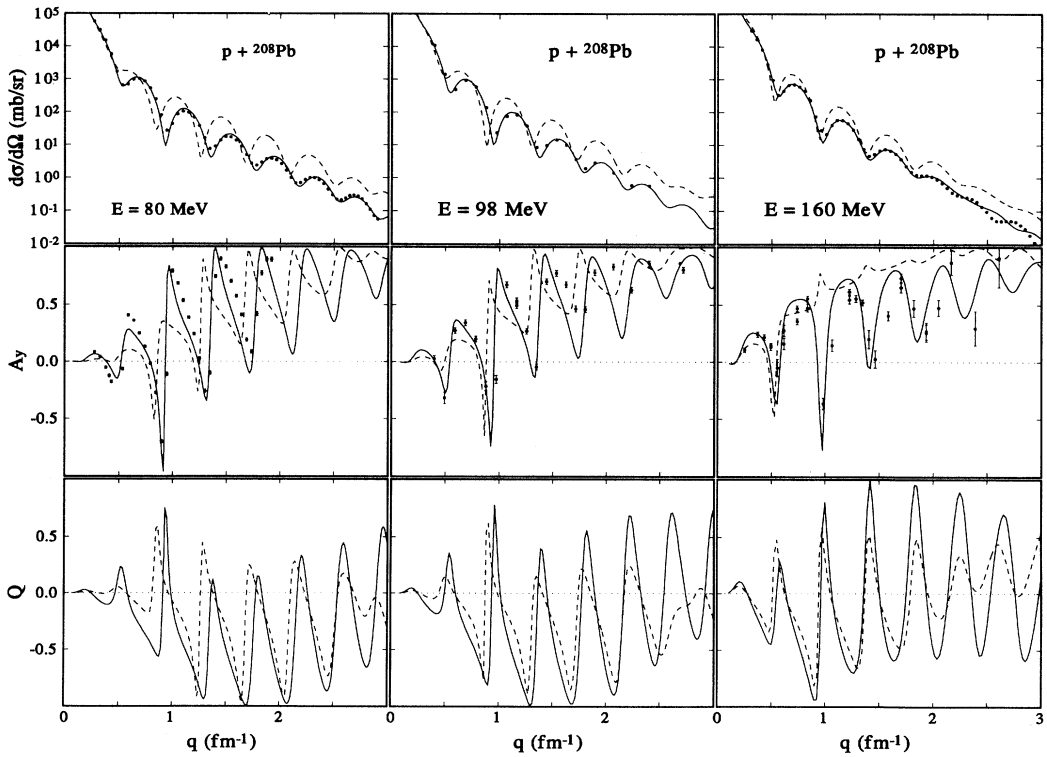

FIG. 7. As in Fig. 3 for p+^{208}Pb elastic scattering at 80, 98, and 160 MeV.

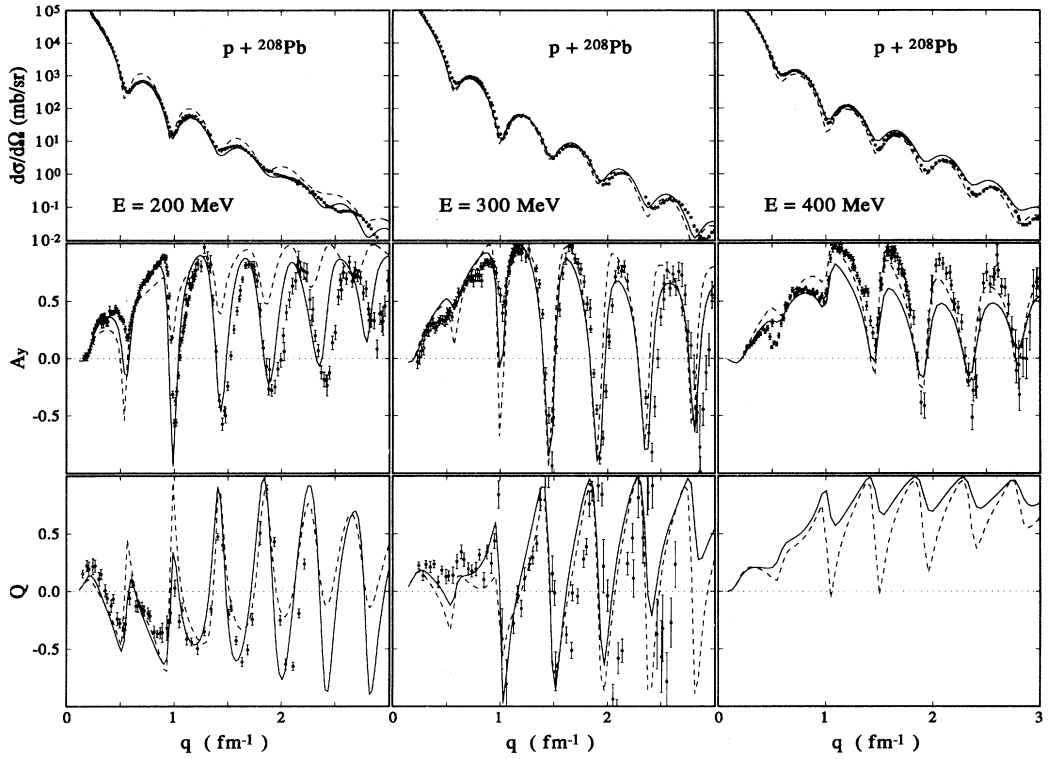

FIG. 8. As in Fig. 3 for p+^{208}Pb elastic scattering at 200, 300, and 400 MeV.

MeV using g matrices with the Pauli function $Q = 1$, namely

$$\lambda_{\vec{P}}^{\rm NM}(\vec{q},\omega;k_F) \to \frac{1}{\omega + i\eta - \epsilon(P_+;k_F) - \epsilon(P_-;k_F)}\ , \quad (47)$$

in Eq. (45) and g matrices which include the Pauli function but with the self-consistent field $U_{\rm NM} = 0$ in the single-particle energy $\epsilon(k;k_F)$, Eq. (17). Thus, the scattering calculations based on the corresponding g matrices should reflect the role of medium effects through its exclusive dependence on the nuclear fields or Pauli blocking, respectively. Results for the corresponding scattering observables are shown in Fig. 9, where we also show results from full-folding calculations based on the full g matrix (solid curves). The dashed curves represent results where the Pauli function is set equal to one. Similarly, the dot-dashed curves represent calculations in which the nuclear

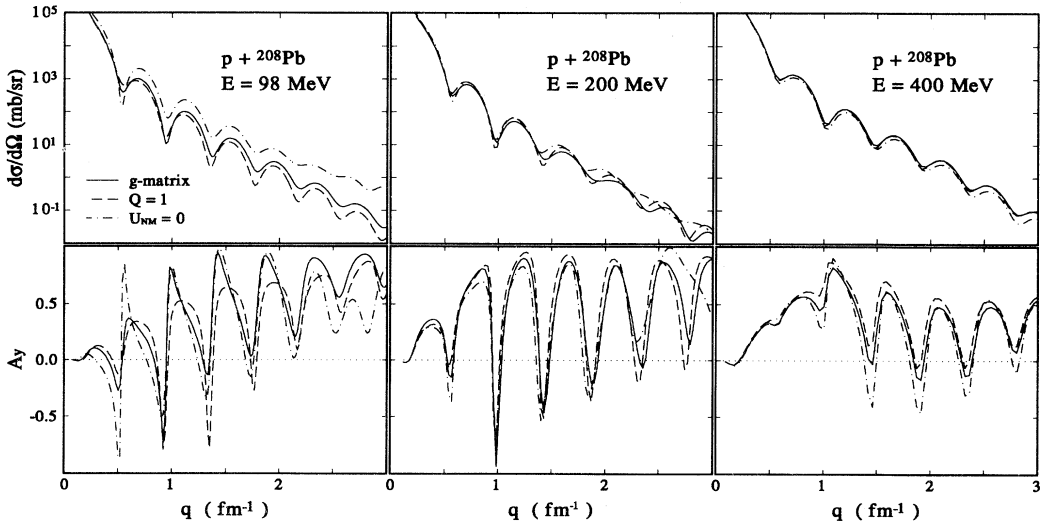

FIG. 9. The effect of Pauli blocking and the nuclear mean field at 98, 200, and 400 MeV in p+^{208}Pb scattering. The solid curves represent complete full-folding calculations with g matrices whereas the dot-dashed and dashed curves represent results obtained setting the nuclear mean field to zero and the Pauli blocking function to unity, respectively.

self-consistent fields are set equal to zero. The scattering data has been omitted. As observed, nuclear medium effects are noticeable at all three energies considered here and become most pronounced at 98 MeV, as expected. The sensitivity of the cross section to the nuclear medium is manifested in the sharpness of the cross sections, with the calculations without Pauli blocking showing sharper diffraction minima relative to the calculations in which the full g matrix is used. At 98 MeV the medium effects are very pronounced in both observables. In this case the omission of the nuclear mean field yields an overestimated cross section relative to both the data and the full g-matrix calculations, a feature which resembles the results obtained with the t matrix in Fig. 7. The omission of Pauli blocking, on the other hand, reduces the cross section, particularly for $q > 1$ fm^{-1}. At 200 MeV the effects of both Pauli blocking and the nuclear mean fields are still noticeable. Again, the sensitivity to these two effects can be seen in both the cross section and analyzing power. This result, combined with the observations made from Figs. 7 and 8 when comparing the g- vs t-matrix approaches in p+^{208}Pb scattering, demonstrate that at 200 MeV neither Pauli blocking nor nuclear mean fields are negligible for describing the scattering process. However, the effect of the real part of the self-energy $U_{\rm NM}$ tends to become less important as the energy increases. Indeed, in Fig. 1 we observe that $\mathrm{Re}[U_{\rm NM}] \approx 0$ for a nucleon with a local momentum $k \approx 4.2$ fm^{-1} or an energy $E \approx 320$ MeV. Thus we expect that the Pauli blocking will be the dominant effect around 300 MeV. At 400 MeV the role of both blocking and the mean field is again sizeable, more in the analyzing power than in the cross section. In this case, the sensitivity to $U_{\rm NM}$ is due to the repulsive character of the mass operator (Fig. 1) at this energy.

The role of medium effects at beam energies above ~400 MeV has also been investigated in the context of both relativistic [40] ($t\rho$-type) and nonrelativistic [10] (local) approaches. These studies also show that medium affects are still significant at these energies. It is also claimed that these effects are more noticeable in the spin observables than in the cross sections. The results shown here are consistent with those findings.

C. Neutron scattering and total cross sections

The subject of microscopic calculations of neutron total cross sections has been an issue of increasing interest lately [11,41–44]. These data provide a source for global comparison between theory and experiments since they cover a wide range of energy and targets and are of a very high quality.

Microscopic calculations of the total cross section for relatively light ($A \leq 40$) systems having $N = Z$ have very recently met with some success [11,44]. Although there has been an extensive analysis of total cross sections based on Dirac phenomenology [43], we are unaware of any recent microscopic calculations for targets with a neutron excess. The simultaneous consideration of both light and heavy nuclei poses a particularly challenging problem. First, the size of the system being studied changes considerably, and second, the isovector part of the NN interaction participates.

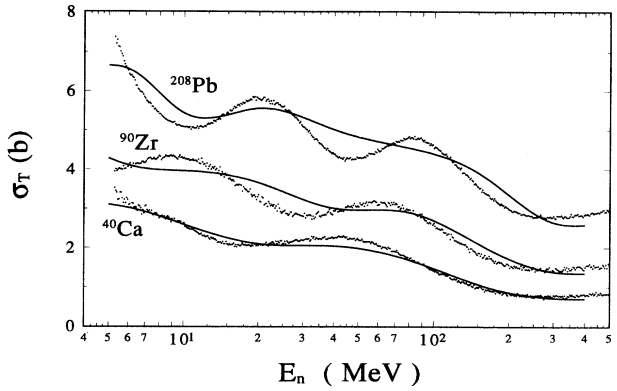

FIG. 10. Measured and calculated (solid lines) total cross sections for neutron scattering from ^{40}Ca, ^{90}Zr, and ^{208}Pb. See text for reference to the data.

In Fig. 10 we present calculations and data [41,45] of total cross sections (σ_T) for neutron scattering from ^{40}Ca, ^{90}Zr, and ^{208}Pb as a function of the neutron incident energy. The solid curves correspond to calculations based on full-folding optical potentials with medium effects treated as described earlier in this paper. It is worth noting that although these full-folding calculations do not describe $\sigma_T(E)$ in detail, they do follow, on average, the energy dependence of the respective data, even at energies as low as 5 MeV. We also observe that for the heavier nuclei, particularly ^{208}Pb, the data exhibit more structure than the calculated σ_T. This feature is different from that exhibited by phenomenological calculations where the cross section is overestimated but its structure is accurately reproduced [43]. We should emphasize that the present calculations include the symmetry potential through the treatment of the folding of the effective force with the neutron and proton densities. In Ref. [43] the neutron σ_T was calculated by simply turning off the Coulomb part of the proton-nucleus potential.

Recent results [44] based on a refined $t\rho$ approach to the optical potential with nuclear medium modifications are in good agreement with experiment for light nuclei. Our findings for ^{40}Ca are of similar quality but over a wider range of energy. We estimate, however, that definite conclusions on the theory cannot be drawn until calculations for heavier nuclei are performed using both approaches. To reinforce this point we show in Fig. 11 the exact total cross sections for neutron scattering off ^{40}Ca and ^{208}Pb (full curves), as in Fig. 10, together with those calculated using the free off-shell t matrix as the effective internucleon force (dashed curves). In both calculations, the presence of the deuteron and its effects on the absorptive part of the optical potential are fully included [5]. For the ^{40}Ca target we observe that both results are relatively close, notably in the 10–50 MeV range. However, there are notable differences above 70 MeV. Our interpretation is that medium effects, and in particular the presence of the nuclear mean field $\mathrm{Re}[U_{\rm NM}]$, generates a shift in energy of the total cross section from the dashed to the full curve as required by the data. This effect is not

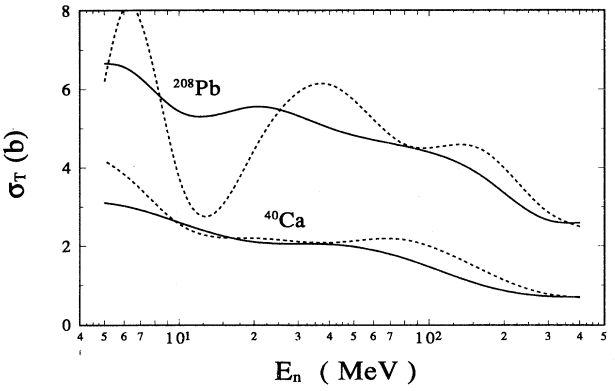

FIG. 11. Calculated total cross sections for neutron scattering from ^{40}Ca and ^{208}Pb. The solid lines represent calculated σ_T from the g matrix as in Fig. 10, and the dashed curves correspond to σ_T obtained using the free t matrix.

seen in the 10–50 MeV range due to the lack of structure in σ_T. For the ^{208}Pb case, the differences between the g- and t-matrix results are significant over the entire energy range considered. The most striking feature is the loss of structure in the total cross section when medium effects are included in the calculation of the effective force, and at present this is not understood. It is clear that the average information about the nuclear medium as provided by symmetric nuclear matter is not sufficiently accurate to give the details of the effective force required to explain these extensive and high-precision data.

V. SUMMARY AND CONCLUSIONS

In this work we have addressed the problem of calculating the optical potential for NA elastic scattering when nuclear medium effects are treated within the full-folding context. In order to achieve this goal we developed a scheme for calculating the effective NN interaction and suggested some plausible approximations to obtain a readily workable model. Our approach provides a general framework for understanding how nucleons interact in the nuclear medium; the range of applicability of the approach can be extended well beyond the NA scattering problem. The effective force was calculated using an interacting infinite nuclear matter model while describing the propagation of particles in the medium, although more realistic, target-specific, models could be used within the same formalism. Nevertheless we are able to account for average medium effects such as Pauli blocking and the nuclear mean field.

The NA optical potential was calculated within the full-folding framework. As a result, we have been able to to treat accurately the off-shell effects and the energy dependence of the effective interaction as prescribed by the Fermi motion of the nucleons in the nucleus. The optical potential takes a relatively simple form, Eq. (43), when we consider an average binding energy for the target nucleons and let the off-shell sampling be driven by the mean bound nucleon momentum $\vec{P}$ in Eq. (36). We believe that the latter approximation needs to be tested in more detail although it requires a considerable amount of extra computing effort.

Nonrelativistic full-folding calculations of the optical potential which include medium corrections were made for p+^{40}Ca and p+^{208}Pb elastic scattering at energies between ~30 and 400 MeV. Scattering observables obtained from these calculations were compared with full-folding calculations based on the free t matrix to describe the NN effective interaction. The differences between these two approaches show that medium effects are significant over the entire range of energies studied in this work (30–400 MeV). Since all calculations presented here treat the off-shell contributions accurately and on the same footing, the differences in the scattering observables between the two models for the NN interaction can be attributed exclusively to medium effects. Furthermore, since no localization procedure is carried out to construct a simpler effective interaction, we have been able to isolate sources of sensitivity of elastic scattering observables obtained from the corresponding optical potentials.

On the other hand, we have observed that applications of the medium-corrected full-folding calculations presented here are qualitatively superior in the case of proton scattering on ^{208}Pb than on ^{40}Ca. This observation is consistent with the closer resemblance that ^{208}Pb has to an extended system than does ^{40}Ca. The nuclear matter two-body propagator we have used for calculating the effective interaction is less justifiable at the surface of the nucleus than in its volume due to the fact that the range of the nuclear correlations is comparable to the diffuseness of the nucleus at the surface. Furthermore, as the volume of the nucleus increases, the fraction of volume contributions increase relative to the surface ones. This observation and the assumption of the dominance of one-step processes should favor applications for heavier systems.

We have also investigated the relative importance of medium effects by studying the sensitivity of scattering observables to Pauli blocking and the nuclear mean field. We observe that these two aspects play a noticeable role over the full range of energies considered here. Although medium effects at 400 MeV seem to be less important than at the lower energies, the scattering observables are still visibly affected by the inclusion of blocking and the mean fields.

The calculation of total cross sections and comparison with the data for neutron scattering from ^{40}Ca, ^{90}Zr, and ^{208}Pb provided another interesting test of the microscopic optical potential, now in the 5–400 MeV energy range. The average magnitude of the total cross section, as a function of the energy, is well reproduced. However, the data show more structure than the calculations as the mass (and size) of the target and therefore its neutron excess increase.

Overall we conclude that the medium corrected full-folding calculations provide a quite reasonable description of the elastic scattering data at energies between 30 and 400 MeV for proton scattering on ^{40}Ca and ^{208}Pb and total cross section data for neutron scattering between 5 and 400 MeV. Difficulties do remain, however, in

the description of spin observables at momentum transfers below ~ 1 fm^{-1}. These difficulties were also noted in previous studies based on full-folding calculations of the optical potential using the free NN t matrix to represent the NN effective interaction. The origin of these discrepancies is not well understood. Apparently some effects are either missing or misrepresented. Some of these could be attributed to the bare internucleon force we use (Paris potential) especially at the higher energies considered, or to the simplified, nuclear matter based, effective NN interaction we calculate. Others effects may require going beyond the first order model discussed here. In any case, the model we have developed and the calculations we have presented constitute a suitable starting point from which further corrections can be investigated.

ACKNOWLEDGMENTS

This work was supported in part by NSF Grants Nos. PHY-8903856 and PHY-9143465 and FONDECYT Grants Nos. 1931115 and 3940008. F.A.B. thanks the Department of Physics and Astronomy of the University of Georgia for its hospitality during his visit.

[1] L. Ray, G. W. Hoffmann, and W. R. Coker, Phys. Rep. **212**, 223 (1992).
[2] Ch. Elster, T. Cheon, E. F. Redish, and P. C. Tandy, Phys. Rev. C **41**, 814 (1990).
[3] R. Crespo, R. C. Johnson, and J. A. Tostevin, Phys. Rev. C **41**, 2257 (1990).
[4] H. F. Arellano, F. A. Brieva, and W. G. Love, Phys. Rev. Lett. **63**, 605 (1989); Phys. Rev C **41**, 2188 (1990).
[5] H. F. Arellano, F. A. Brieva, and W. G. Love, Phys. Rev. C **50**, 2480 (1994).
[6] A. Picklesimer, P. C. Tandy, R. M. Thaler, and D. H. Wolfe, Phys. Rev. C **30**, 1861 (1984).
[7] F. A. Brieva and J. R. Rook, Nucl. Phys. **A291**, 317 (1977); **A307**, 493 (1978).
[8] H. V. von Geramb, in *The Interaction Between Medium Energy Nucleons in Nuclei*, edited by H. O. Meyer (AIP, New York, 1983).
[9] L. Rikus and H. V. von Geramb, Nucl. Phys. **A426**, 496 (1984).
[10] L. Ray, Phys. Rev. C **41**, 2816 (1990).
[11] C. R. Chinn, Ch. Elster, and R. M. Thaler, Phys. Rev. C **48**, 2956 (1993).
[12] R. Crespo, R. C. Johnson, and J. A. Tostevin, Phys. Rev. C **48**, 351 (1993).
[13] G. R. Satchler, in *Direct Nuclear Reactions* (Oxford University Press, New York, 1983).
[14] A. L. Fetter and K. M. Watson, in *Advances in Theoretical Physics*, edited by K. A. Brueckner (Academic, New York, 1965), Vol. 1.
[15] Leo P. Kadanoff and Gordon Baym, in *Quantum Statistical Mechanics* (Addison-Wesley, Reading, MA, 1989).
[16] J. P. Jeukenne, A. Lejeune, and C. Mahaux, Phys. Rep. C **25**, 83(1976).
[17] John W. Negele and Henri Orland, in *Quantum Many-Particle Systems* (Addison-Wesley, Reading, MA, 1988).
[18] H. Feshbach, Ann. Phys. (N.Y.) **5**, 357 (1958); **19**, 287 (1962).
[19] A. K. Kerman, H. McManus, and R. M. Thaler, Ann. Phys. (N.Y.) **8**, 551 (1959).
[20] H. F. Arellano, W. G. Love, and F. A. Brieva, Phys. Rev. C **42**, 652 (1990).
[21] X. Campi and A. Bouyssy, Phys. Lett. **73B**, 263 (1978).
[22] M. Lacombe, B. Loiseau, J. M. Richard, R. Vinh Mau, J. Côté, P. Pirés, and R. de Tourreil, Phys. Rev. C **21**, 861 (1980).
[23] S. K. Adhikari and K. L. Kowalski, in *Dynamical Collision Theory and Its Applications* (Academic, New York, 1991).
[24] N. Yamaguchi, S. Nagata, and T. Matsuda, Prog. Theor. Phys. **70**, 459 (1983).
[25] A. Lejeune, P. Grangé, M. Marazolff, and J. Cugnon, Nucl. Phys. **A453**, 189 (1986).
[26] A. A. Ioannides and R. C. Johnson, Phys. Rev. C **17**, 1331 (1978).
[27] J. W. Negele, Phys. Rev. C **1**, 1260 (1970).
[28] B. W. Ridley and J. F. Turner, Nucl. Phys. **54**, 497 (1964)
[29] R. M. Craig, J. C. Dore, G. W. Greenlees, J. S. Lilley, and J. Lowe, Nucl. Phys. **54**, 515 (1964).
[30] R. H. McCamis *et al.*, Phys. Rev. C **33**, 1624 (1986).
[31] L. N. Blumberg, E. E. Gross, A. van der Woude, A. Zucker, and R. H. Bassel, Phys. Rev. **147**, 812 (1966).
[32] H. Sakaguchi, M. Nakamura, K. Hatanaka, A. Goto, T. Noro, F. Ohtani, H. Sakamoto, H. Ogawa, and S. Kobayashi, Phys. Rev. C **26**, 944 (1982); B. C. Clark (private communication).
[33] A. Nadasen, P. Schwandt, P. P. Singh, W. W. Jacobs, A. D. Bacher, P. T. Debevec, M. D. Kaitchuck, and J. T. Meek, Phys. Rev. C **23**, 1023 (1981).
[34] P. Schwandt, H. O. Meyer, W. W. Jacobs, A. D. Bacher, S. E. Vidgor, M. D. Kaitchuck, and T. R. Donoghue, Phys. Rev. C **26**, 55 (1982).
[35] A. Ingemarsson and G. Tibell, Phys. Scr. **4**, 235 (1971).
[36] E. J. Stephenson, J. Phys. Soc. Jpn. (Suppl.) **55**, 316 (1985).
[37] D. A. Hutcheon *et al.*, Nucl. Phys. **A483**, 429 (1988).
[38] E. Bleszynski *et al.*, Phys. Rev. C **37**, 1527 (1988).
[39] W. T. H. van Oers, H. Haw, and N. E. Davison, Phys. Rev. C **10**, 307 (1974).
[40] D. P. Murdock and C. J. Horowitz, Phys. Rev. C **35**, 1442 (1987).
[41] R. W. Finlay, W. P. Abfalterer, G. Fink, E. Montei, T. Adami, P. W. Lisowski, G. L. Morgan, and R. C. Haight, Phys. Rev. C **47**, 237 (1993).
[42] Yanhe Jin and R. W. Finlay, Phys. Rev. C **47**, 1697 (1993).
[43] E. D. Cooper, S. Hama, B. C. Clark, and R. L. Mercer, Phys. Rev. C **47**, 297 (1993).
[44] C. R. Chinn, Ch. Elster, R. M. Thaler and S. P. Weppner, Phys. Rev. C **51**, 1033 (1995).
[45] R. W. Finlay, G. Fink, W. P. Abfalterer, P. W. Lisowski, G. L. Morgan and R. C. Haight, in *Proceedings of the International Conference on Nuclear Data for Science and Technology*, edited by S. M. Qaim (Springer-Verlag, Berlin, 1992).